Traveling waves and pulses in a two-dimensional large-aspect-ratio system

M. Bestehorn and H. Haken
Institut für Theoretische Physik and Synergetik, Universität Stuttgart, Pfaffenwaldring 57/4, D-7000 Stuttgart 80, Germany
(Received 9 July 1990)

Near a bifurcation point a system far from thermal equilibrium can be described by use of generalized Ginzburg-Landau equations. We present a systematic method to derive the nonlinear interaction terms of these equations in real space reflecting the selection rules as well as the stabilization of different patterns intrinsic in the basic equations of the systems under consideration. Our work treats the case of periodic instabilities of a homogeneous state in space as well as in time, where the interacting patterns are represented by traveling-wave trains having arbitrary orientations in a two-dimensional plane. Numerical solutions of two-dimensional pattern formation and wave propagation are presented using a system that allows for a backward Hopf bifurcation as is the case for the convection instability of a binary fluid mixture. The stability of the emerging traveling-wave structures is discussed in terms of phase-diffusion equations.

I. INTRODUCTION

In the vicinity of a phase transition the spatiotemporal behavior of a system far from thermal equilibrium can be described very often by a few relevant variables that in analogy to the Ginzburg-Landau theory of equilibrium thermodynamics, are called "order parameters." The large number of state variables originally assigned to the dynamics of the system under consideration and present in its basic equations of motion can be expressed by the order parameters in a unique way. The elimination of the enslaved modes allows a drastic reduction of the complexity of the system.[1-3]

The purpose of the present paper is to show the connection of the explicit form of an order-parameter equation (OPE) in real space, especially of its nonlinearities, with the structure of a nonlinear expansion of the basic equations into Fourier modes. If these modes are determined as being solutions of the linearized basic equations, e.g., the hydrodynamic equations for the convection instability, the OPE can be derived from first principles. In some other cases where the basic equations are not completely known, the OPE can be discussed as a phenomenological model for pattern formation, e.g., in chemistry or biology (for reviews, see, e.g., Refs. 4–6).

The paper is organized as follows. We first establish general relations between the cubic coupling in Fourier space and real space, which will be finally used to derive a partial differential equation allowing for the selection of traveling or standing waves in a rotationally invariant form with respect to two dimensions. In particular, we investigate the case of a Hopf bifurcation of a spatially structured pattern from a spatiotemporally homogeneous state. Then we numerically treat this equation for several cubic coupling models were fronts, pulses, and traveling waves are formed. We also study effects of a subcritical bifurcation where the OPE has to be at least of fifth order. A simple physical system showing an oscillatory (backward) bifurcation of a spatially periodic state is realized, for instance, by the convection instability of a binary mixture and examined intensively both experimentally and theoretically in the last ten years (see, e.g., Refs. 7–9). Despite the fact that for this system the validity of the OPE is restricted and cannot, for instance, describe a secondary bifurcation of the traveling-wave patterns for larger Rayleigh numbers as was shown in Ref. 10, the OPE seems to be able to reflect at least qualitatively the main features of the instability of traveling waves in the weak nonlinear regime near the critical point, such as the selection of traveling waves instead of standing waves or the behavior of fronts between regions of waves having different directions of propagation.

If the dynamics is restricted to one spatial dimension there is a close analogy to the formalism of amplitude equations first considered by Newell and Whitehead.[11] However, this formalism has the disadvantage that it cannot be extended to two spatial dimensions in a rotationally invariant form, since each direction of propagation requires an extra envelope equation of the corresponding wave. To avoid this problem, we shall investigate pattern formation by means of the OPE, where the order parameter contains the fully spatiatemporal dynamics on a fast varying scale. In this sense the work of Swift and Hohenberg[12] can be considered as pioneering. They regarded a model that can be applied for the (steady) convection instability. In contrast to this equation, which reflects mainly effects of a rotationally invariant linear selection and which has the simplest possible stabilizing cubic term, our models include spatial derivatives in the nonlinearities as well as complex quantities in the linear part. The latter reflect the coupling, scattering, and selection of interacting wave trains having different directions of propagation. Therefore it becomes possible to describe the formation and the propagation of traveling waves as well as their differentiated interaction in terms of a nonlinear selection mechanism in real space.

II. THE ORDER-PARAMETER EQUATION IN FOURIER SPACE

We consider a system described by an infinite number of order parameter $\xi(\mathbf{k},t)$ that denote the amplitudes of plane waves with the two-dimensional wave vectors $\mathbf{k}$. If the system is isotropic in real space, the linear part of the OPE may only depend on k^2, i.e., the unstable modes lie on a ring in Fourier space with radius k_c. The OPE for those amplitudes reads

$$\dot{\xi}(\mathbf{k},t)=\lambda(k^2)\xi(\mathbf{k},t)+\int d\mathbf{k}_1 d\mathbf{k}_2 d\mathbf{k}_3 \Gamma(\mathbf{k}_1,\mathbf{k}_2,\mathbf{k}_3)\xi(\mathbf{k}_1)\xi(\mathbf{k}_2)\xi^*(\mathbf{k}_3)\delta(\mathbf{k}-\mathbf{k}_1-\mathbf{k}_2+\mathbf{k}_3)$$
$$+\int d\mathbf{k}_1 d\mathbf{k}_2 d\mathbf{k}_3 d\mathbf{k}_4 d\mathbf{k}_5 \Lambda(\mathbf{k}_1,\mathbf{k}_2,\mathbf{k}_3,\mathbf{k}_5)\xi(\mathbf{k}_1)\xi(\mathbf{k}_2)\xi(\mathbf{k}_3)\xi^*(\mathbf{k}_4)\xi^*(\mathbf{k}_5)\delta(\mathbf{k}_1-\mathbf{k}_2-\mathbf{k}_3+\mathbf{k}_4+\mathbf{k}_5)\ , \tag{1}$$

where δ denotes the delta function. Here we assumed inversion symmetry for the order parameter, which results in only odd powers of ξ in (1). We include nonlinearities up to fifth order in ξ, since we want to discuss also the case of a backward bifurcation leading to a positive cubic coefficient Γ for certain mode couplings. We now make the basic assumption that the mode amplitudes ξ near threshold are excited essentially only in a narrow circular band in 2D k space, i.e., on a ring with radius k_c and width Δk. Introducing polar coordinates k and φ we may express the two-dimensional vector $\mathbf{k}$ solely by its orientation φ. Then the first δ function in expression (1) requires a coupling of the four wave vectors $\mathbf{k}$, $\mathbf{k}_1$, $\mathbf{k}_2$, and $\mathbf{k}_3$, forming a rhomb. Therefore the cubic part in (1) may be written as

$$(k_c\Delta k)^3\int_0^{2\pi} d\varphi'[f_1(\varphi-\varphi')\xi(\varphi)|\xi(\varphi')|^2 + f_2(\varphi-\varphi')\xi^*(\varphi+\pi)\xi(\varphi')\xi(\varphi'+\pi)]\ , \tag{2}$$

where

$$f_1(\varphi-\varphi')=\Gamma(\varphi',\varphi,\varphi')+\Gamma(\varphi,\varphi',\varphi')\ ,$$
$$f_2(\varphi-\varphi')=\Gamma(\varphi',\pi+\varphi',\varphi+\pi)\ . \tag{3}$$

Due to the condition of isotropy in real space, the functions f_i may only depend on the relative angle between $\mathbf{k}$ and $\mathbf{k}'$. If we assume that Γ contains scalar products of its arguments $\mathbf{k}_i$, we may approximate f_i by a Taylor series with respect to $\cos(\varphi-\varphi')$ along

$$f_1(\beta)=\sum_{n=0}^{N} a_n(\cos\beta)^n,\quad f_2(\beta)=\sum_{n=0}^{N/2} b_{2n}(\cos\beta)^{2n}\ . \tag{4}$$

Because of the symmetry with respect to $\varphi'\mapsto\varphi'+\pi$ in the second expression under the integral (2), odd powers of $\cos\beta$ cancel in f_2 and only even powers have to be taken into account.

III. THE ORDER-PARAMETER EQUATION IN REAL SPACE

Now we wish to derive the analog to (1) in real space. If we make the assumptions of the last section which finally led to (2), we end up with a partial differential equation without any nonlocal expressions. Let $\Psi(\mathbf{x},t)$ be the inverse Fourier transform of the order parameter $\xi(\mathbf{k},t)$. In the linear part of the OPE we allow for a variation of the wave vector in a band centered at k_c. It can be approximated in real space by

$$\lambda^u(\varepsilon,\Delta)\approx\varepsilon+i\omega_c-g^2(k_c^2+\Delta)^2-i\gamma(k_c^2+\Delta)\ . \tag{5}$$

For a steady bifurcation ($\omega_c=\gamma=0$), (5) is reduced to the linear part of the well-known Swift-Hohenberg equation[12] which was numerically treated in two spatial dimensions in Ref. 13 as a model of the convection instability. The angular dependence of the third-order term may be approximated by spatial derivatives, or, with regard to a rotationally invariant formulation of the problem, by powers of the 2D Laplacian. If we consider for the cubic term the general expression

$$\Psi^*\sum_{n=0}^{N}\frac{A_n}{k_c^{2n}}(-\tfrac{1}{2}\Delta-k_c^2)^n\Psi^2+\Psi\sum_{n=1}^{N}\frac{B_n}{k_c^{2n}}(-\tfrac{1}{2}\Delta-k_c^2)^n|\Psi|^2 \tag{6}$$

and if we assume again a finite bandwidth excitation of the mode amplitudes, the relation between A_n,B_n,a_n,b_n of formulas (4) and (6) may be established as follows:

$$a_0=2A_0+\sum_{n=1}^{N}(-1)^nB_n\ ,$$
$$a_n=2A_n+(-1)^nB_n,\quad n=1,2,3,\ldots$$
$$b_0=\sum_{n=0}^{N}(-1)^nA_n\ , \tag{7}$$
$$b_n=B_n,\quad n=2,4,6,\ldots\ .$$

(7) enables us to express the fully angular dependence intrinsic in (1) of the mode coupling between wave trains with given arbitrary orientation via the local form (6) including only rotationally invariant expressions of spatial derivatives. The only restriction in our derivation is the reduction of the excited band to its critical value k_c, therefore our model can describe only qualitatively sideband instabilities where the instability mechanism is due to the growth of a disturbance having a different absolute value of the wave vector and not of the orientation in real space.

The fifth-order term in (1) can be expressed by the same procedure in a local form, however due to the coupling of six wave vectors there are three free angles in the corresponding expression in Fourier space allowing for a much more complex behavior of mode coupling.

IV. NUMERICAL SOLUTIONS: FRONTS

In our numerical simulations we chose for the cubic nonlinearity the lowest truncation with respect to powers

of Δ, which still enables us to differentiate the coupling strength between waves having different directions, i.e., $A_0, B_1, \neq 0$ in (6). Therefore we establish the complex OPE for a spatiotemporal instability having the wavelength 2π and the frequency ω_c:

$$\dot{\Psi}(\mathbf{x},t)=\{\varepsilon-g^2(1+\Delta)^2+i[\omega_c-\gamma(1+\Delta)]\}\Psi(\mathbf{x},t) + A_0\Psi(\mathbf{x},t)|\Psi(\mathbf{x},t)|^2-B_1\Psi(\mathbf{x},t)|\nabla\Psi(\mathbf{x},t)|^2 + C|\Psi(\mathbf{x},t)|^4\Psi(\mathbf{x},t) . \quad (8)$$

For the sake of global stability, we added a fifth-order term having a stabilizing sign ($\mathrm{Re}C<0$). This allows us also to include subcritical bifurcations where A_0 or B_1 can act in a destabilizing way. The angular-dependent part of the cubic term simplifies to

$$f_1(\beta)=2A_0-B_1-B_1\cos\beta .$$

In one spatial dimension, the ratio of the real parts of A_0 and B_1 determines the selection of traveling or standing waves. The one-dimensional coupled equations for their amplitudes (see Ref. 14) η and ζ read

$$\dot{\eta}=[\varepsilon+v\partial_x+D\partial_{xx}+(A_0-B_1)|\eta|^2+2A_0|\zeta|^2 + C(6|\zeta|^2|\eta|^2+3|\zeta|^4+|\eta|^4)]\eta ,$$
$$\dot{\zeta}=[\varepsilon-v\partial_x+D\partial_{xx}+(A_0-B_1)|\zeta|^2+2A_0|\eta|^2 + C(6|\zeta|^2|\eta|^2+3|\eta|^4+|\zeta|^4)]\zeta . \quad (9)$$

Since we are interested in pattern formation in two spatial dimensions, we shall not consider (9) further but focus our attention on (8). We performed a numerical treatment of (8) in a circular as well as in a quadratic layer using a pseudospectral method and a semi-implicit time integration scheme. For the order parameter Ψ we assumed the boundary conditions

$$\Psi=\partial_n\Psi=0 , \quad (10)$$

where $\mathbf{n}$ is oriented vertically to the boundary. First we examined the case where all nonlinear coefficients in (8) were real valued and $C=-1$. As an initial condition, we used patterns where only small (singular) centers of the layer have a nonvanishing wave function, whereas Ψ was set to zero on the rest of the layer. Due to the rotation symmetry of our equations, the pattern development starts always with circular or spiral rings, depending on the initial distribution in the centers. These rings have the wavelength $\lambda_c=2\pi$ and travel with the phase velocity $v_{\mathrm{ph}}=\omega_c$. The envelope of each center thereby propagates radially until it encounters an obstacle such as the wall or another wave front. We studied this evolution both subcritically as well as supercritically. The cross-coupling term A_0 becomes important in the moment where two wave trains confront at any part of the layer. Here we investigated the influence of the self-coupling term A_0-B_1 for the case of a small negative cross coupling. Figure 1 shows the situation for a negative self-coupling of the same magnitude as the cross coupling. The waves can penetrate after collision and no formation or stabilization of a front between counterpropagating wave trains can be seen. This changes dramatically if the self-coupling expression becomes positive (Fig. 2). Now a front is created between the centers. However, the front is not stable and moves towards the initially somewhat smaller region. The same behavior is obtained for a cubic OPE having stabilizing (negative) self- as well as cross-coupling coefficients. If A_0 is increased further, the emerging front has a larger slope and turns out to be stable against fluctuations or nonsymmetric initial conditions (see Fig. 3). Next we performed time series for the same parameter values for very large aspect ratios, starting now with different kinds of centers (Fig. 4). The "ring type" has azimuthal symmetry; the "spiral type" has an angular dependence according to $\exp\pm i\varphi$ in the initial states. The time series presented in Fig. 4 shows the emergence and stabilization of fronts between several domains of radially traveling waves. Note that there is no essential difference between the dynamics of circular rings or spa-

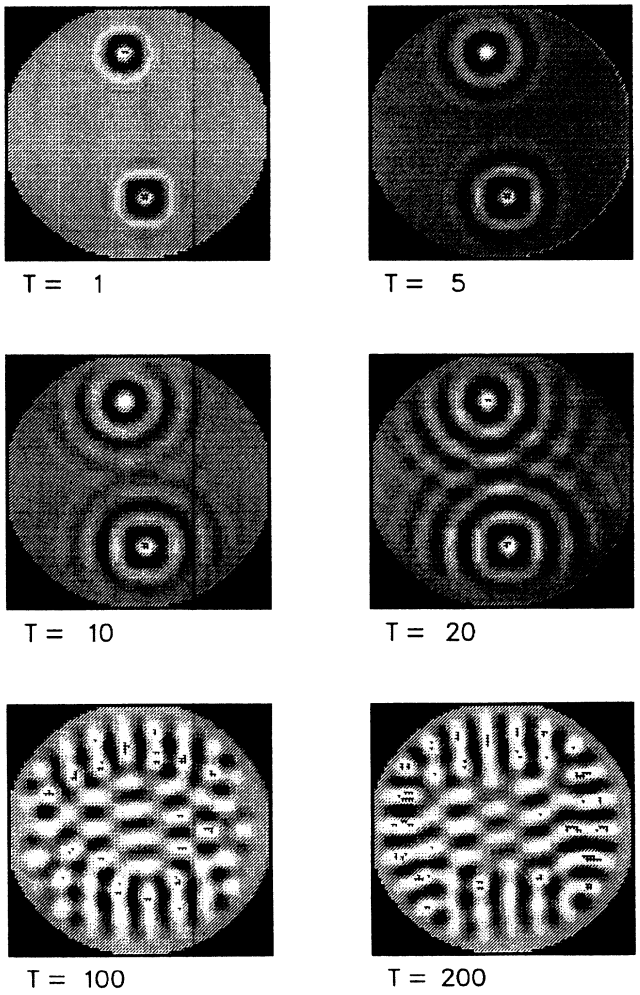

FIG. 1. Numerical solutions of (8) for real nonlinear coefficients and a negative self-coupling A_0-B_1. The initial condition consists of two domains with nonzero values for Ψ and $\Psi=0$ for the rest of the plane. The circles are spread out in the form of propagating rings. Where they collide, they penetrate each other.

tials, both types expand with about the same velocity and have the same properties with respect to their ability of forming stable regions and fronts between them. This fact corresponds to the degeneracy of the propagation of plane waves in a 2D medium with respect to their orientation.

V. NUMERICAL SOLUTIONS: TRAVELING WAVES AND PULSES

We now investigate the case where the cubic and quintic coefficients have nonvanishing imaginary parts. In earlier publications[15] we gave solutions of (8) with cubic coefficients that allow for the supercritical formation of traveling waves for the case of a binary mixture having idealized vertical boundaries. These wave trains were unstable with respect to long-wavelength instabilities, the Benjamin-Feir instability,[16] and a chaotic spatiotemporal behavior emerged already at onset. Here we wish to focus our attention on the propagation and stabilization of subcritical 2D pulses, in analog to recent analytical and numerical 1D results[17,18] of the slowly varying amplitude truncation of (8) where pulses were stabilized for a considerably large parameter region. However, compared to the wavelength of the underlying periodic pattern enveloped by these pulses, the amplitude is not slowly varying in space and the envelope equation cannot be regarded as an approximation of (8). In fact, the stable pulses found in Ref. 18 have the extension of about one critical wavelength 2π of (8). A numerical calculation of (8) using the complex coefficients where stable pulses have been found in Ref. 18, namely $\varepsilon=-0.1$, $A_0=3+i$, $B_1=0$, $C=-2.75+i$ shows immediately that pulses being stable in the second-order truncated amplitude equation begin now to travel in the opposite (e.g., left) direction of the phase velocity of the underlying (right) traveling-wave structure ($\gamma=0$). We may say that the inclusion of higher derivatives in the amplitude equation as well as the direct solution of the OPE allows still for the existence of pulses that, in contrast to the second-order

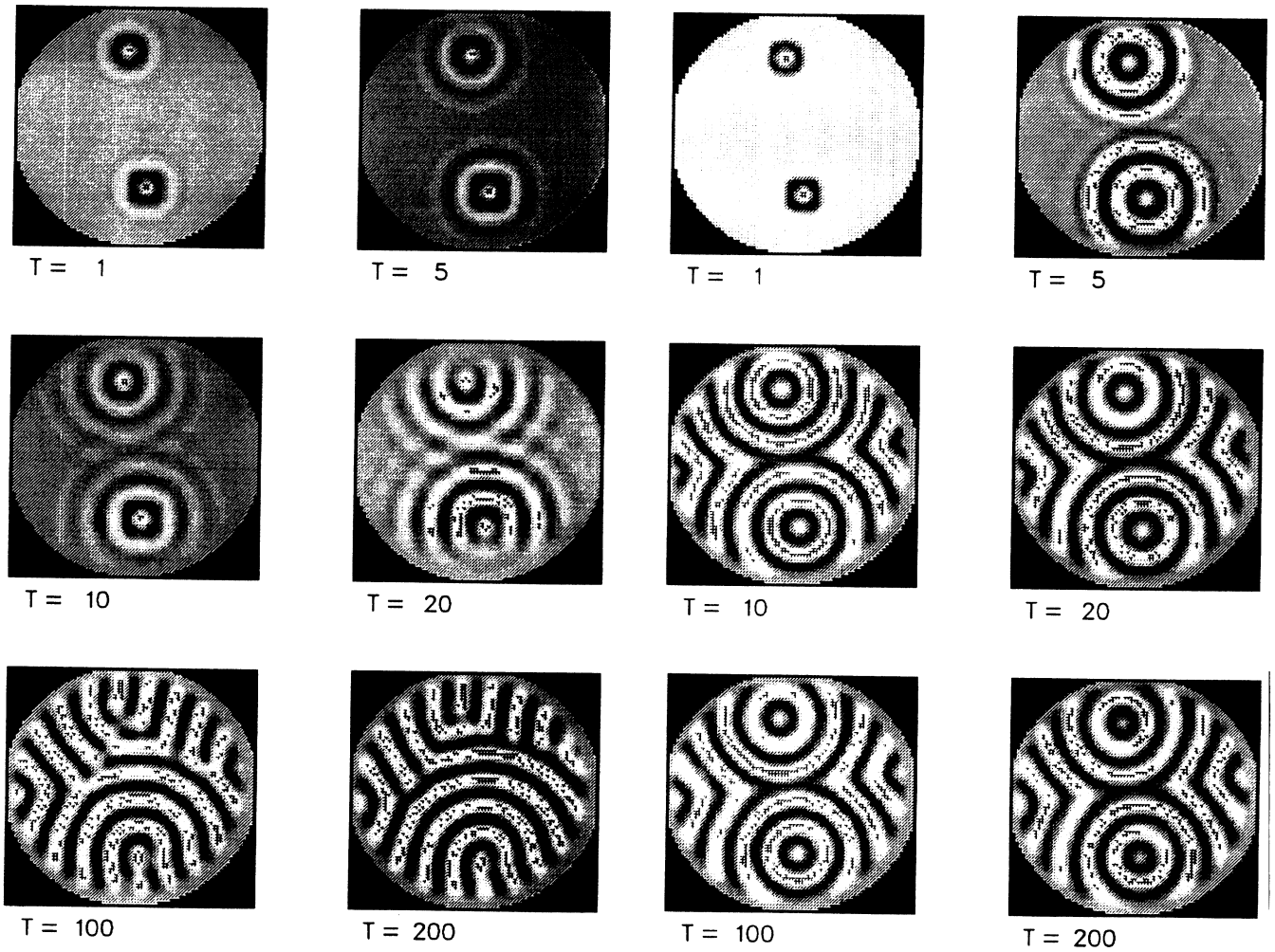

FIG. 2. Same as Fig. 1, but for slightly positive values of A_0-B_1. Now the fronts are formed in the colliding regions, which are not stable but move towards the center with a somewhat smaller initial amplitude.

FIG. 3. Same as Fig. 1, but for large positive A_0-B_1. The front between the centers is stabilized.

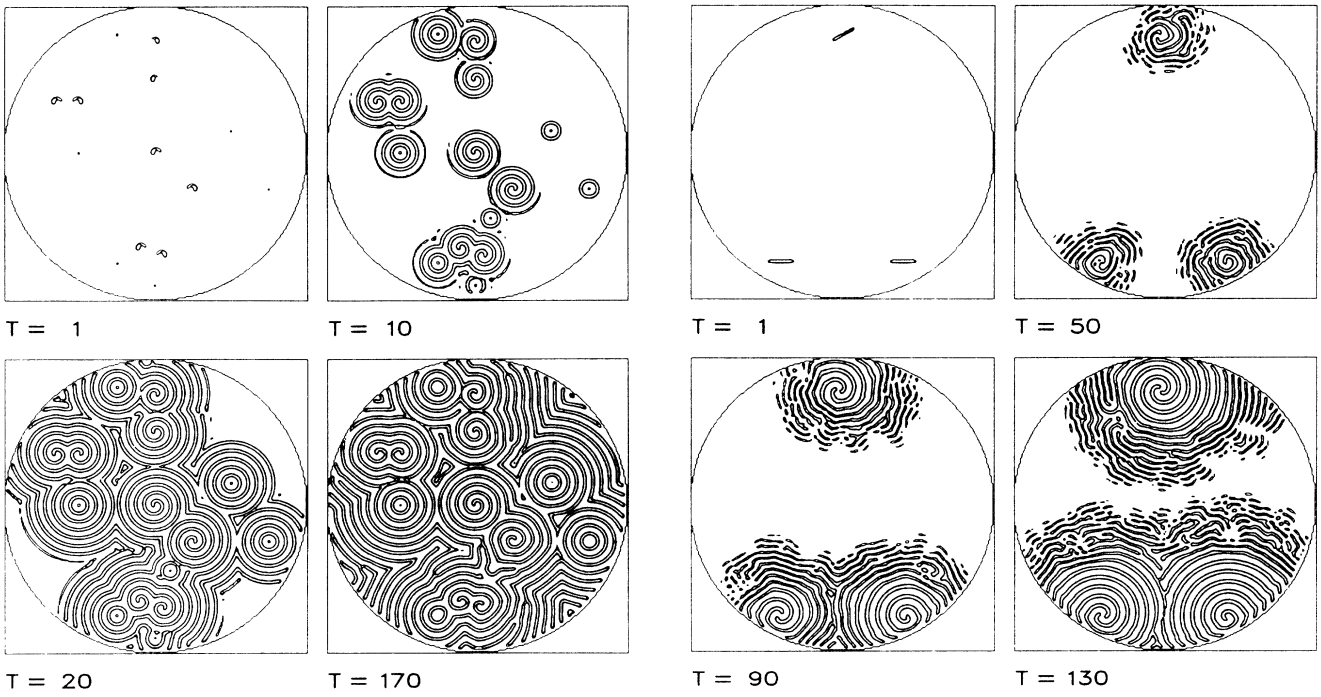

FIG. 4. Same as Fig. 3, but for a spatially more extended system. The initial conditions are now rings and spirals with azimuthal dependence $\exp \pm i\varphi$. Smaller domains are unstable with respect to larger ones. The domain walls at $T=170$ are stable. All domains consist of circular or rotating spiral wave traveling towards the lateral wall.

FIG. 6. Subcritical time development of three pulses in a large layer. Cubic destabilizing term without spatial derivatives. $\gamma=0.3$. The pulses are unstable and form after some transient spirals that do not penetrate. $A_0=3+i$, $B_1=0$, $C=-2.75+i$, $\varepsilon=-0.1$. Due to the fast frequency ω_c, the spirals are rotating counterclockwise (bottom left and top) or reverse (bottom right).

truncation examined in Ref. 18, propagate generically in one direction. This behavior is even more complex in two spatial dimensions. Since the problem has to be formulated rotationally invariant, we apply the OPE (8) using again the complex coefficients of Ref. 18 in a nonlinear representation first without any spatial derivatives. It seems that transversal instabilities that can be controlled by the dispersion γ now play a crucial role (the following section). We first set $\gamma=-0.3$. As an initial condition we chose a pulse that consists of a short train

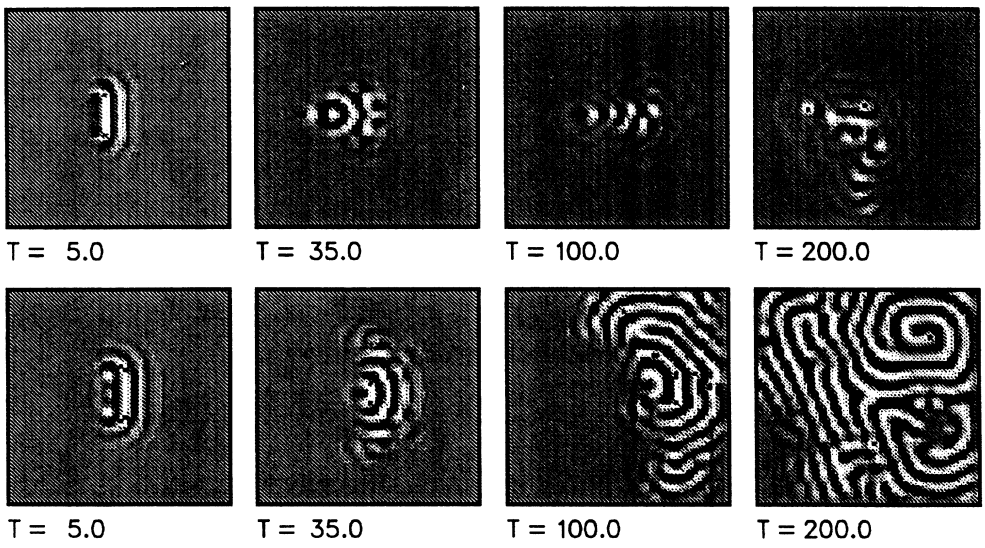

FIG. 5. Subcritical time development of a pulse in two dimensions, with a cubic destabilizing term without spatial derivatives. For negative γ, the pulse stays localized. $A_0=3+i$, $B_1=0$, $C=-2.75+i$, $\varepsilon=-0.1$. Top, $\gamma=-0.3$; bottom; $\gamma=0.3$.

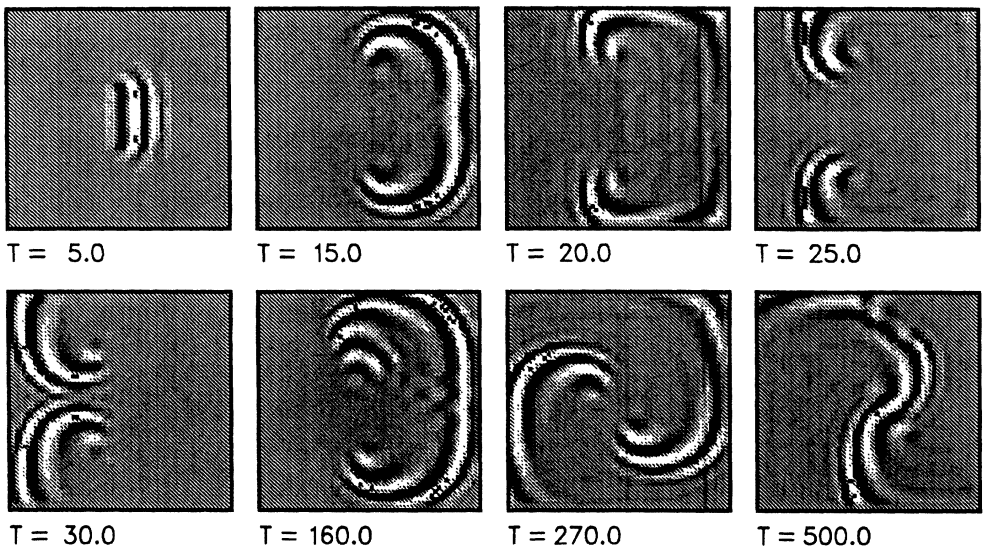

FIG. 7. Same as Fig. 5 but with spatial derivatives in the cubic term. $\gamma=0.6$. The fronts are reflected by the boundaries $A_0=0$, $B_1=-3-i$, $C=-2.75+i$, $\varepsilon=-0.1$.

(one critical wavelength) of traveling waves to the right and that is localized using a Gaussian envelope vertical to its wave vector. Figure 5 (top) shows a time series of the first 200 time units. The pulse is getting wider in the x direction but does not essentially change its central position. In the y direction, wave trains perpendicular to the initial waves are generated on the edges of the primary waves via a transverse instability. In contrast to solutions for $\gamma=0.3$ (see Fig. 5, bottom, and Fig. 6) the pulse is still localized in two dimensions.

The creation of secondary-wave trains and the destabilization of a pulse for positive γ is more evident if spatial derivatives in the cubic expression are included that account for a faster propagation in the direction of the wave vector of the primary waves (Fig. 7). The secondary waves are formed after $t=5$ and form themselves tertiary waves and so on leading finally to a sort of spiraling. All wave fronts move to the outside and are reflected by the sidewalls. We mention that these states are strongly time dependent and the system shows no tendency to settle down to a stationary state in the time limit of our simulations. The series in Fig. 8 is for a much larger aspect ratio where the influence of the sidewalls becomes less important. The annihilation of counterpropagating wave trains in the bulk now becomes clearly visible. This is due to the fact that counterpropagating waves couple with a vanishing cubic coefficient by our choice of A_0 and B_1. Confronting waves therefore bifurcate supercritically and are consequently damped for negative ε. This annihilation is in accordance with the numerical 1D calculations in Ref. 18, where colliding pulses erase each other for certain parameter values.

Figure 9 shows the stabilization and very slow propagation of a sharp 2D pulse starting with the same initial condition as in Fig. 8 but for negative γ. Finally, Fig. 10 shows the evolution for the same parameters for a larger aspect ratio starting with a random dot pattern. Narrow wave trains are formed at $T=130$ and travel in a radial direction direction towards the center of the layer where they erase each other. This is accordance with calculations based on the linearized problem (8) together with the boundary conditions (10) and is caused by a phase

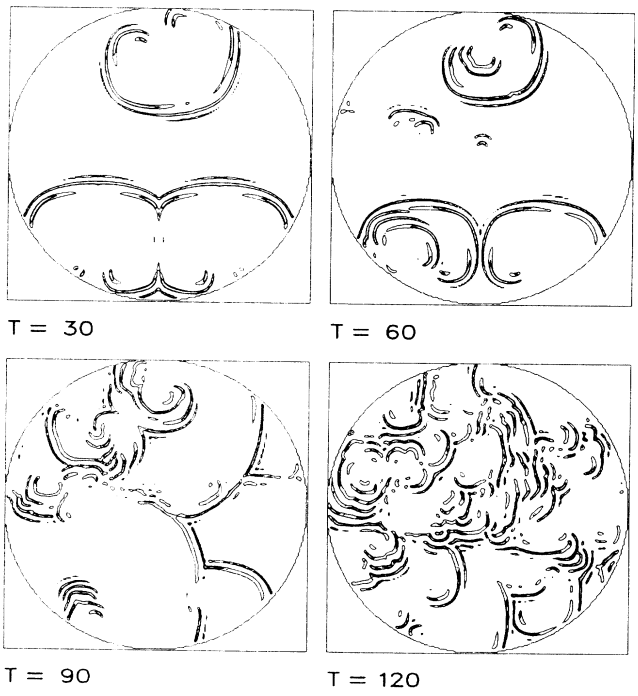

FIG. 8. Time development in a large circular layer. Wave fronts that collide erase each other and vanish. Same coefficients as in Fig. 7.

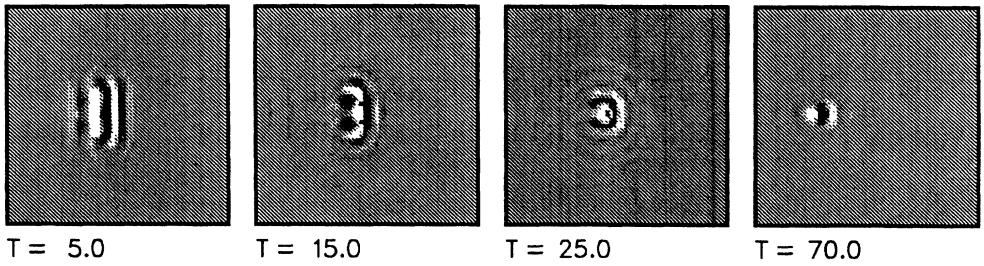

FIG. 9. Formation of a pulse via a transversal instability of a wave front with a cubic destabilizing term including spatial derivatives. $\gamma=-0.6$.

shift between the real and imaginary parts of the order parameter near the sidewall.[19]

VI. PHASE INSTABILITIES

The region of stability of a traveling-wave solution with wave vector k in (8) can be achieved using the technique of phase equations.[20] The ansatz

$$\Psi(\mathbf{x},t)=[Q_k+\delta Q(\mathbf{x},t)]\exp\{i[\Omega_k-kx+\Phi(\mathbf{x},t)]\} \quad (11)$$

inserted in (8) leads, after linearization with respect to Φ and δQ followed by an adiabatic elimination of δQ, to a diffusion equation for the phase of the form

$$\dot{\Phi}(\mathbf{x},t)=(v_D\partial_x+D_{\parallel}\partial_{xx}+D_{\perp}\partial_{yy})\Phi(\mathbf{x},t) \quad (12)$$

with the diffusion constants

$$D_{\parallel}=2g^2(3k^2-1)+\frac{2\alpha_k(\alpha_k+kB_1'Q_k)}{Q_k^2(A_0'+2C'Q_k^2-k^2B_1')}-\gamma\gamma_k\ , \quad (13)$$

$$D_{\perp}=2g^2(k^2-1)-\gamma\gamma_k\ , \quad (14)$$

and the drift velocity

$$v_D=2\gamma k+2\gamma_k(B_1'kQ_k-\alpha_k)-2B_1''kQ_k\ . \quad (15)$$

We used the abbreviations

$$\gamma_k=\frac{A_0''+2C''Q_k^2-k^2B_1''}{A_0'+2C'Q_k^2-k^2B_1'}\ ,$$

$$\alpha_k=-2g^2k(k^2-1)\ ,$$

$$A_0=A_0'+iA_0''\ ,$$

etc. for B_1, C. Q_k^2 is the larger root of the equation

$$\varepsilon-g^2(1-k^2)^2+(A_0'-B_1'k^2)Q_k^2+C'Q_k^4=0\ . \quad (16)$$

The zeros of the diffusion coefficients $D_{\parallel}, D_{\perp}$ mark the onset of the longitudinal and the transversal instability, respectively, in the ε-k plane (see Figs. 11 and 12). For negative γ the wave vector having the largest linear growth rate is unstable due to the transversal instability for both coefficient settings and the region of stability shrinks to zero with decreasing γ. It seems possible that this instability leads to a collapse of the wave front and to the formation of pulses after which the phase diffusion, Eq. (12), is no longer valid. For positive γ the stability region of a traveling wave is much larger and the numerical results show finally a pattern that fills the whole layer and that is far from being localized (see, e.g., Fig. 6). During the propagation shown in Fig. 6, the waves that emerge at the fronts have a considerably smaller wavelength than those in the regular centers of the spirals and fall probably in the longitudinally unstable region of the

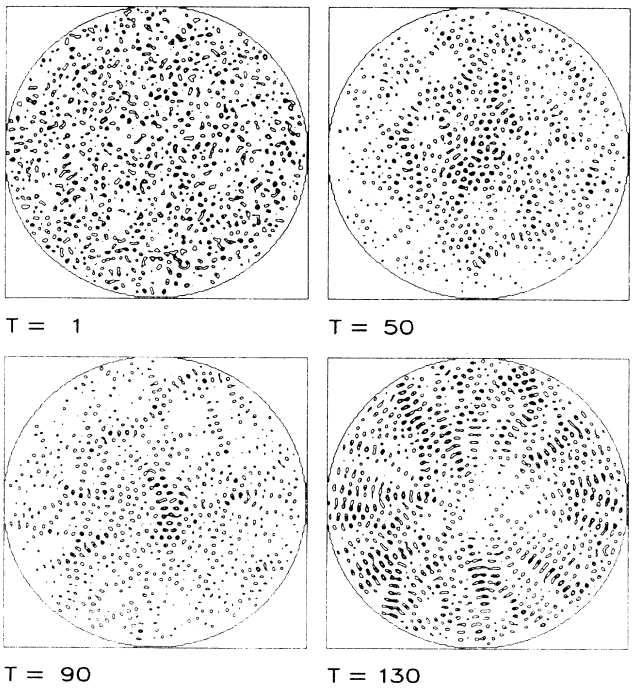

FIG. 10. Same as Fig. 9, but with a random initial condition in a large aspect ratio.

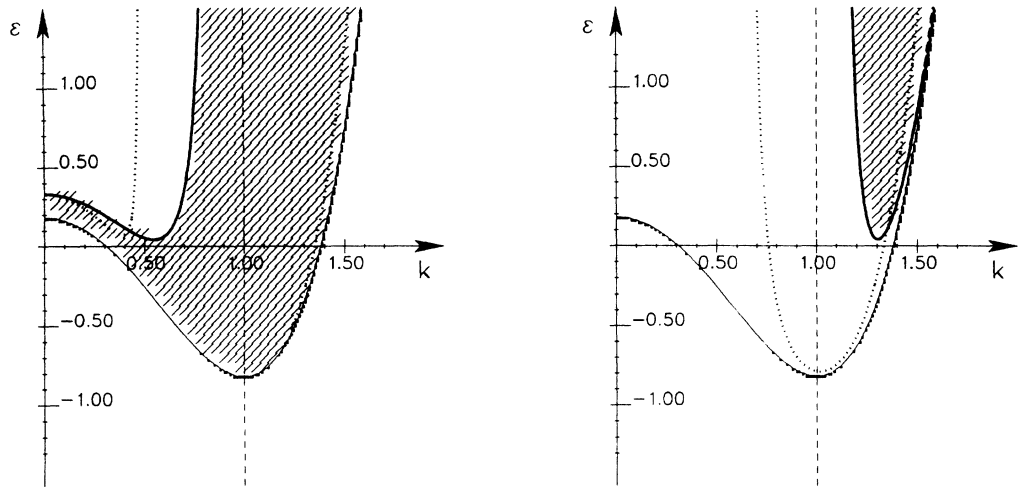

FIG. 11. Stability diagram for a traveling wave with wave vector k of (8). The coefficients were $g=1$, $A_0=3+i$, $B_1=0$, $C=-2.75+i$, $\gamma=1$ (left), and $\gamma=-1$ (right). In the shaded areas, both diffusion coefficients in (12) are positive and the traveling-wave solution is stable. Dashed curve, longitudinal instability; solid curve, transversal instability; dashed vertical line, critical k.

phase. Far behind the front the wavelength expands into the stable region of Fig. 11, left.

VII. CONCLUSION

We have presented a method to calculate the nonlinear expressions of the order-parameter equations including rotationally invariant derivatives in two spatial dimensions. These equations can reflect the main features of mode coupling and selection of the basic equations of the problems under consideration, e.g., convection in binary mixtures or reaction diffusion problems. However, if the variation of the envelopes of the plane waves vary on a short length scale compared to the critical wavelength of the underlying patterns, the approximation of the reduction of the excited band to a ring in Fourier space is no longer valid and new effects can occur, such as the longitudinal breakdown of a continuous roll pattern to some isolated localized traveling fronts. This happens if the cubic coefficients have nonvanishing imaginary parts and the spatial derivatives near a front can create modes outside the critical ring.

On the other hand, if the dispersion is assumed to be negative, a continuous roll pattern collapses, probably due to a transversal phase instability into 2D pulses.

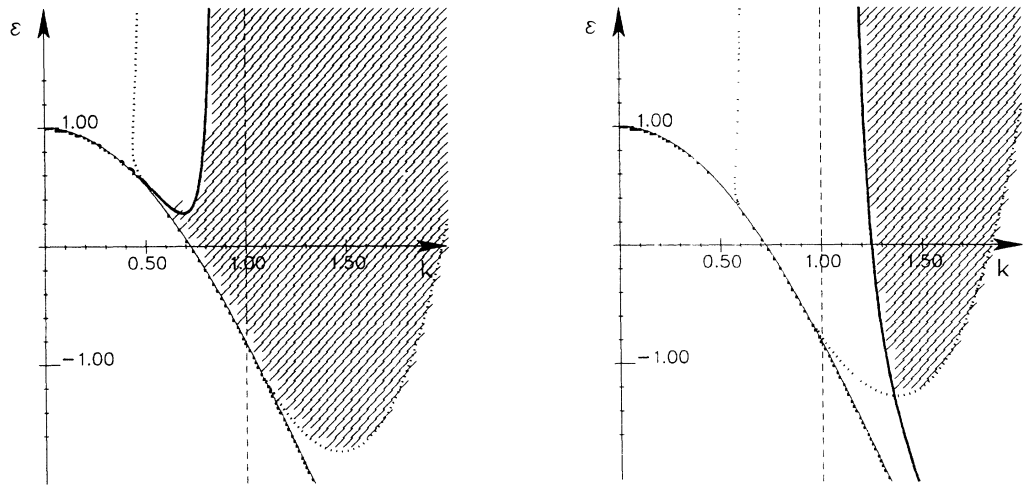

FIG. 12. Same as Fig. 5, but with the coefficients $A_0=0$, B_1-3-i, $C=-2.75+i$, $\gamma=1$ (left), and $\gamma=-1$ (right).

ACKNOWLEDGMENTS

We gratefully acknowledge helpful discussions with Dr. R. Friedrich. We thank Dr. H. Ohno and A. Fuchs for useful advice on the Cray II of the Computer Center of the University of Stuttgart (RUS). Finally, we wish to thank the Volkswagenwerk foundation, Hannover, for financial support within the project on synergetics.

[1]H. Haken, *Synergetics. An Introduction,* 3rd ed. (Springer, Berlin, 1983).

[2]H. Haken, *Advanced Synergetics,* (Springer, Berlin, 1987).

[3]H. Haken, Rep. Prog. Phys. **52**, 515 (1989).

[4]Y. Kuramoto, *Chemical Oscillations, Waves, and Turbulence,* Vol. 19 of *Springer Series in Synergetics* (Springer, Berlin, 1984).

[5]N. F. Britton, *Reaction-Diffusion Equations and Their Applications to Biology* (Academic, London, 1986).

[6]J. D. Murray, *Mathematical Biology* (Springer, Berlin, 1989).

[7]V. Steinberg, E. Moses, and J. Fineberg, Nucl. Phys. B **2**, 109 (1987).

[8]D. Gutkowicz-Krusin, M. A. Collins, and J. Ross, Phys. Fluids **22**, 1443 (1979); **22**, 1457 (1979).

[9]J. K. Platten and J. C. Legros, *Convection in Liquids* (Springer, Berlin, 1984).

[10]D. Bensimon, A. Pumir, and B. I. Shraiman, J. Phys. (France) **50**, 3089 (1989).

[11]A. C. Newell and J. A. Whitehead, J. Fluid. Mech. **38**, 279 (1969); A. C. Newell, in *Propagation in Systems Far from Equilibrium,* Vol. 41 of *Springer Series in Synergetics,* edited by J. E. Wesfreid, H. R. Brand, P. Manneville, G. Albinet, and N. Boccara (Springer, Berlin, 1988).

[12]J. Swift and P. C. Hohenberg, Phys. Rev. A **15**, 319 (1977).

[13]H. S. Greenside, W. M. Coughran, Jr., and N. L. Schreyer, Phys. Rev. Lett. **49**, 729 (1982); H. S. Greenside and W. M. Coughran, Jr., Phys. Rev. A **30**, 398 (1984).

[14]M. C. Cross, Phys. Rev. Lett. **57**, 2935 (1986).

[15]M. Bestehorn, R. Friedrich, and H. Haken, Z. Phys. B **75**, 265 (1989); **77**, 151 (1989); Physica **D37**, 295 (1989).

[16]T. B. Benjamin and J. E. Feir, J. Fluid Mech. **27**, 417 (1967).

[17]W. van Saarlos and P. C. Hohenberg, Phys. Rev. Lett. **64**, 749 (1990).

[18]H. R. Brand and R. J. Deissler, Phys. Rev. Lett. **63**, 280 (1989).

[19]M. Bestehorn (unpublished).

[20]Y. Pomeau and P. Manneville, J. Phys. (Paris) **42**, 1067 (1981); H. R. Brand, P. S. Lombdahl, and A. C. Newell, Phsica D **23**, 345 (1986).

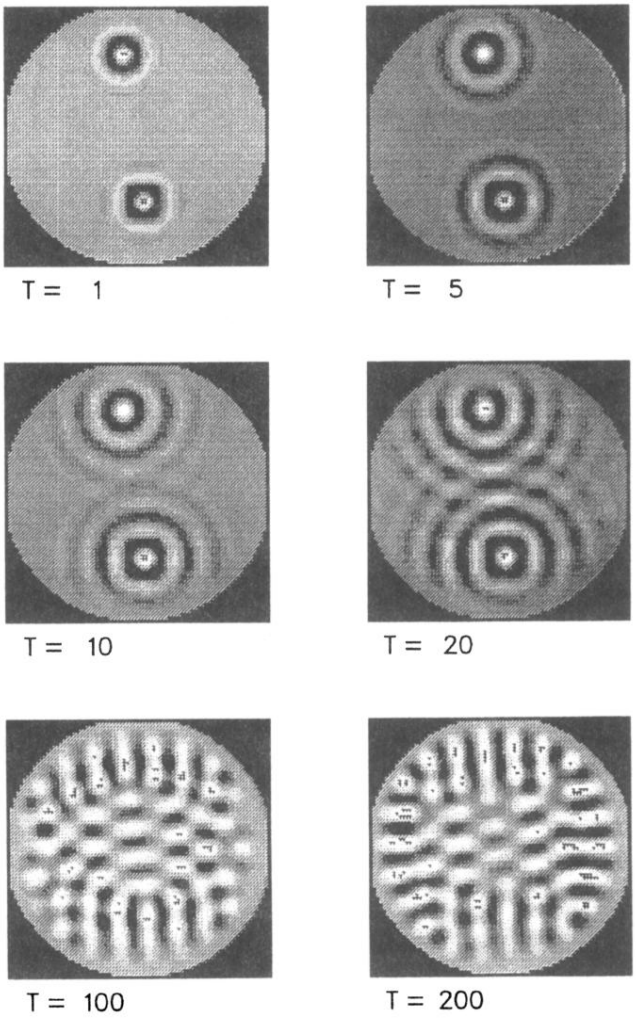

FIG. 1. Numerical solutions of (8) for real nonlinear coefficients and a negative self-coupling $A_0 - B_1$. The initial condition consists of two domains with nonzero values for Ψ and $\Psi = 0$ for the rest of the plane. The circles are spread out in the form of propagating rings. Where they collide, they penetrate each other.

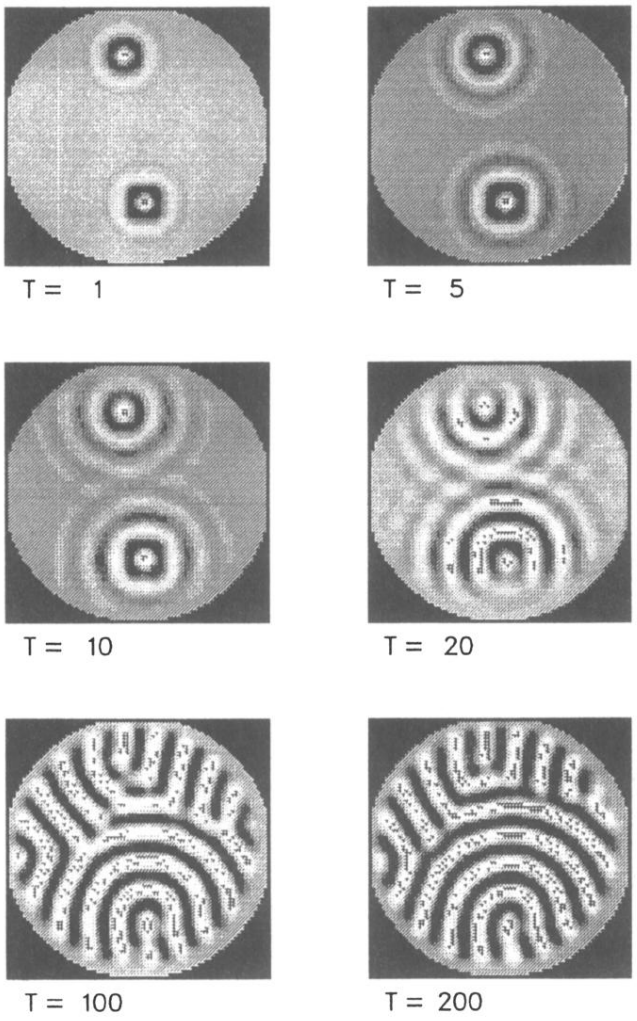

FIG. 2. Same as Fig. 1, but for slightly positive values of $A_0 - B_1$. Now the fronts are formed in the colliding regions, which are not stable but move towards the center with a somewhat smaller initial amplitude.

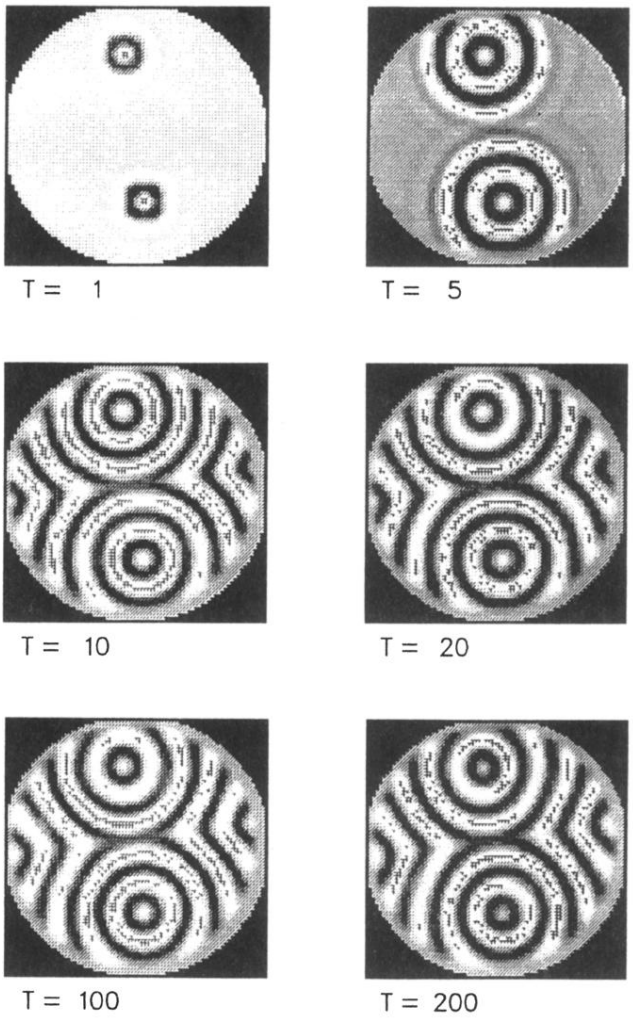

FIG. 3. Same as Fig. 1, but for large positive $A_0 - B_1$. The front between the centers is stabilized.

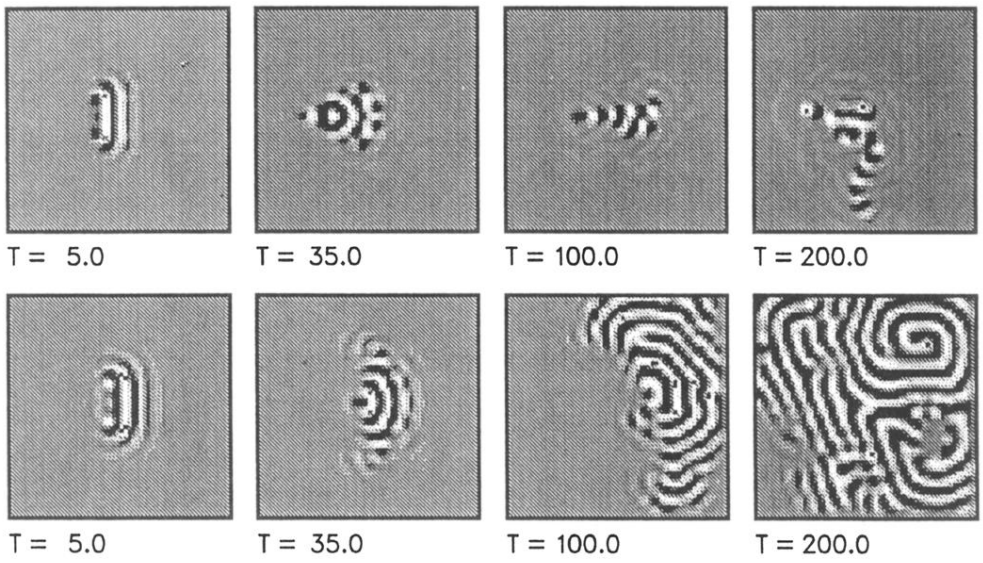

FIG. 5. Subcritical time development of a pulse in two dimensions, with a cubic destabilizing term without spatial derivatives. For negative γ, the pulse stays localized. $A_0=3+i$, $B_i=0$, $C=-2.75+i$, $\varepsilon=-0.1$. Top, $\gamma=-0.3$; bottom; $\gamma=0.3$.

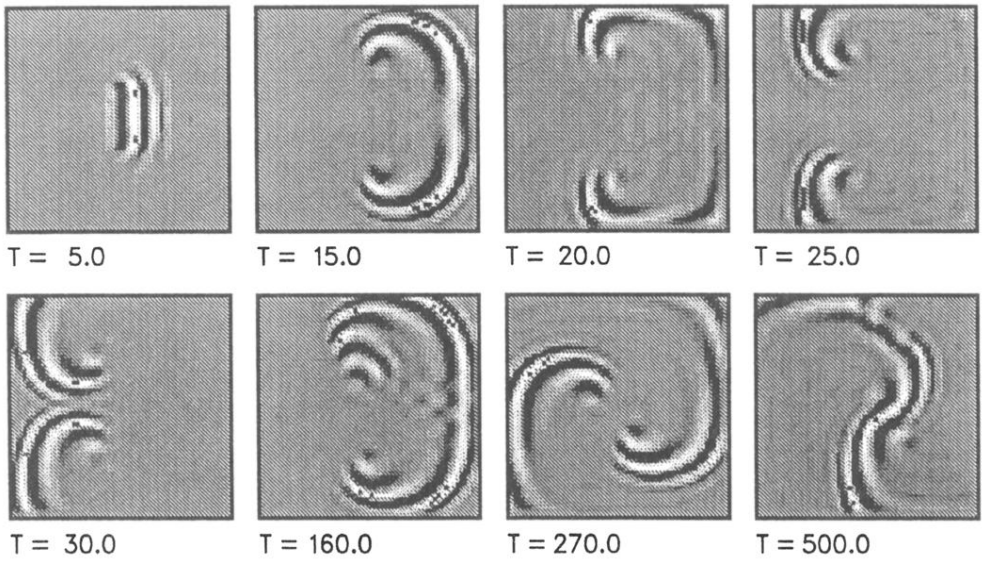

FIG. 7. Same as Fig. 5 but with spatial derivatives in the cubic term. $\gamma=0.6$. The fronts are reflected by the boundaries $A_0=0$, $B_1=-3-i$, $C=-2.75+i$, $\varepsilon=-0.1$.

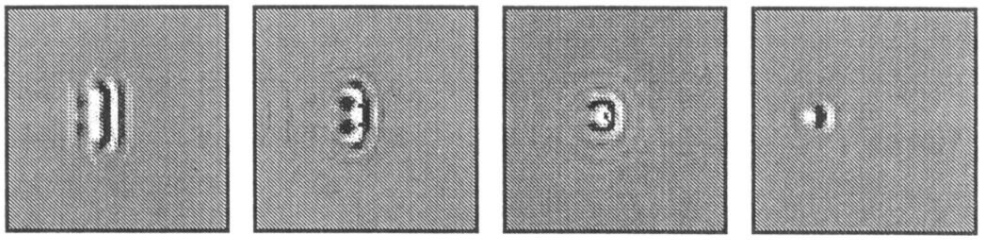

FIG. 9. Formation of a pulse via a transversal instability of a wave front with a cubic destabilizing term including spatial derivatives. $\gamma = -0.6$.